Research Article | Vol. 24, No. 23 | 14 Nov 2016 | OPTICS EXPRESS 26332

Optics EXPRESS

Simplified modeling and optimization of silicon modulators based on free-carrier plasma dispersion effect

D. PÉREZ-GALACHO,[1,*] D. MARRIS-MORINI,[1] R. STOFFER,[2] E. CASSAN,[1] C. BAUDOT,[3] T. KORTHORST,[2] F. BOEUF,[3] AND L. VIVIEN[1]

[1]*Center for Nanoscience and Nanotechnology, CNRS, Univ. Paris-Sud, Universite Paris-Saclay, C2N-Orsay, 91405 Orsay Cedex, France*
[2]*PhoeniX BV, Hengelosestraat 705, 7521 PA Enschede, The Netherlands*
[3]*ST Microelectronics, 850 rue Jean Monnet, 38920 Crolles, France*
[*]*diego.perez-galacho@u-psud.fr*

Abstract: In this paper, a simplified model of silicon phase modulators is presented that enables favorable accuracy together with a substantial reduction in computational effort and without the requirement of semiconductor TCAD device simulation software. This permits fast optimization of the different parameters of a modulator. The model was successfully implemented in Phoenix Optodesigner optical software allowing the optimization of silicon phase shifters for different applications. Moreover, this model presents a great potential for the simulation of modulators based on PN interdigitated junctions, which normally require complex and time consuming 3D simulations. Simulation time was reduced by a factor of 6 for the lateral PN junction based modulator, and two orders of magnitude reduction was obtained for interdigitated PN junctions based modulators.

OCIS codes: (130.4110) Modulators; (130.0250) Optoelectronics; (130.0130) Integrated optics; (130.3120) Integrated optics devices.

References and links

1. T.-Y. Liow, J. Song, X. Tu, A.-J. Lim, Q. Fang, N. Duan, M. Yu, and G.-Q. Lo, "Silicon optical interconnect device technologies for 40 gb/s and beyond," IEEE J. Sel. Topics Quantum Electron. **19**, 8200312 (2013).
2. G. T. Reed, G. Z. Mashanovich, F. Y. Gardes, M. Nedeljkovic, Y. Hu, D. J. Thomson, K. Li, P. R. Wilson, S.-W. Chen, and S. S. Hsu, "Recent breakthroughs in carrier depletion based silicon optical modulators," Nanophotonics **3**, 229–245 (2014).
3. F. Yang, Y. He, W. Chen, and Y. Zhan, "Laser altimeter based on random code phase modulation and heterodyne detection," IEEE Photon. Technol. Lett. **26**, 2337–2340 (2014).
4. T. Baba, S. Akiyama, M. Imai, N. Hirayama, H. Takahashi, Y. Noguchi, T. Horikawa, and T. Usuki, "50-gb/s ring-resonator-based silicon modulator," Opt. Express **21**, 11869–11876 (2013).
5. K. Kajikawa, T. Tabei, and H. Sunami, "An infrared silicon optical modulator of metal–oxide–semiconductor capacitor based on accumulation-carrier absorption," Jpn. J. Appl. Phys. **48**, 04C107 (2009).
6. D. Marris-Morini, L. Virot, C. Baudot, J.-M. Fédéli, G. Rasigade, D. Perez-Galacho, J.-M. Hartmann, S. Olivier, P. Brindel, P. Crozat, F. Boeuf and L. Vivie, "A 40 gbit/s optical link on a 300-mm silicon platform," Opt. Express **22**, 6674–6679 (2014).
7. T. Ando, "Optical coherent beam control based on microwave photonics technologies," in "Microwave Photonics (MWP) and the 2014 9th Asia-Pacific Microwave Photonics Conference (APMP), 2014 International Topical Meeting on," (IEEE, 2014), pp. 381–384.
8. P. Ma, Y. Lü, P. Zhou, X. Wang, Y. Ma, and Z. Liu, "Investigation of the influence of mode-mismatch errors on active coherent polarization beam combining system," Opt. Express **22**, 27321–27338 (2014).
9. G. Rasigade, D. Marris-Morini, M. Ziebell, E. Cassan, and L. Vivien, "Analytical model for depletion-based silicon modulator simulation," Opt. Express **19**, 3919-3924 (2011)
10. R. A. Soref and B. Bennett, "Electrooptical effects in silicon," IEEE J. Quantum Electron. **23**, 123–129 (1987).
11. M. A. Webster, K. Lakshmikumar, C. Appel, C. Muzio, B. Dama, and K. Shastri, "Low-power MOS-capacitor based silicon photonic modulators and CMOS drivers," in Optical Fiber Communication Conference, OSA Technical Digest (online) (Optical Society of America, 2015), paper W4H.3.
12. A. Jüngel, "Drift-diffusion equations," in *Transport Equations for Semiconductors*, (Springer, 2009).
13. K. Iizuka, *Elements of Photonics, vol. II. For Fiber and Integrated Optics*, B. Saleh, ed. (John Wiley & Sons, 2002).

#278803 http://dx.doi.org/10.1364/OE.24.026332
Journal © 2016 Received 14 Oct 2016; revised 20 Oct 2016; accepted 20 Oct 2016; published 4 Nov 2016

Optics EXPRESS

14. F. Gardes, A. Brimont, P. Sanchis, G. Rasigade, D. Marris-Morini, L. O'Faolain, F. Dong, J.M. Fédéli, P. Dumon, L. Vivien, T.F. Krauss, G.T. Reed and J. Martí, "High-speed modulation of a compact silicon ring resonator based on a reverse-biased pn diode," Opt. Express **17**, 21986–21991 (2009).
15. X. Xiao, H. Xu, X. Li, Z. Li, T. Chu, Y. Yu, and J. Yu, "High-speed, low-loss silicon mach–zehnder modulators with doping optimization," Opt. Express **21**, 4116–4125 (2013).
16. http://www.lumerical.com.
17. Y. Amemiya, H. Ding, and S. Yokoyama, "Design and simulation of silicon ring optical modulator with p/n junctions along circumference," Jpn. J. Appl. Phys. **50**, 04DG13 (2011).
18. Y. Amemiya, R. Furutani, M. Fukuyama, and S. Yokoyama, "Silicon ring optical modulator with p/n junctions arranged along waveguide for low-voltage operation," Jpn. J. Appl. Phys. **51**, 04DG07 (2012).
19. D. Marris-Morini, C. Baudot, J.-M. Fédéli, G. Rasigade, N. Vulliet, A. Souhaité, M. Ziebell, P. Rivallin, S. Olivier, P. Crozat, X. L. Roux, D. Bouville, S. Menezo, F. Bœuf, and L. Vivien, "Low loss 40 gbit/s silicon modulator based on interleaved junctions and fabricated on 300 mm soi wafers," Opt. Express **21**, 22471–22475 (2013).

1. Introduction

Silicon photonics has become nowadays a reference platform for many photonics based applications, including sensing and telecommunications. It benefits from CMOS compatibility, enabling its integration with current microtechnology circuitry. This feature makes it suitable for next generation photonic technologies, including intra- and inter-chip optical interconnects as an example [1]. Silicon phase modulators play a key role in many photonic domains [2], including sensors based on heterodyne detection [3], transmitters [4–6] and coherent beam combining systems [7, 8]. Depending on the application, modulators' specifications are very different. Low loss and high efficiency are common demands in sensing orientated applications. Bandwidth, however, is normally the critical parameter in data communications. Wavelength chirp may also be important in some applications. Optimizing a modulator according to given specifications often requires many simulations during the design stage. However, modulators' simulations typically require a lot of memory and long computation times, hindering the ability of the designer to optimize the modulator in a reasonable time. Modulators modeling is of great importance in order overcome those constraints [9]. In this work we propose a simplified model for silicon modulators that alleviates those constraints, without requiring semiconductor TCAD simulations and while maintaining a good level of accuracy. The proposed model is validated against complete 3D simulations and it has been successfully implemented in Phoenix Optodesigner optical software. Furthermore, we used the model to optimize a modulator that is typically challenging to design, a modulator based on carrier depletion in interdigitated PN junctions.

2. Simplified modeling of phase modulators

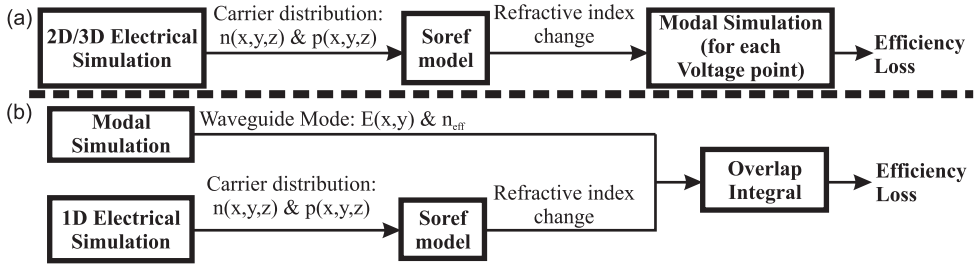

Fig. 1. General schematic of the complete simulation (a) and the simplified phase modulator model (b).

In Fig. 1(a), the general flux diagram of the complete simulation of silicon modulators based on Free-Carrier Plasma Dispersion Effect (FCPD) is represented. This approach is generally

Optics EXPRESS

used to analyze silicon modulators. For each set of modulator parameters (geometry, doping concentrations, applied voltage, ...), it involves complexes 2D or 3D optical and electrical simulations. Soref's equations [10] are used to model the refractive index and absorption coefficient changes due to free carriers distribution. Doping profiles are considered uniform, which is common assumption in the analysis of silicon modulators as several ions implantation steps are usually used to obtain such almost uniform doping profiles. It is important to point out that to properly take into account the effect of carriers the modal simulation should be done with a solver based on Finite Element or Finite Difference discretization schemes with a really fine mesh (~ 5nm), requiring large simulation times. However, the use of a simplified model for phase modulators permits the reduction of the memory requirements and simulation time, maintaining a fairly good level of accuracy at the same time. A simplified model for silicon modulator has been presented previously [9] where both the carrier distribution and optical mode distributions were simplified to an analytic expression varying only in one dimension. We propose here an improved simplified modeling of silicon modulator, where the optical mode is simulated in a rigorous way, while the carrier density distribution is simplified to a 1D distribution. This allows the simulation of modulators with complex mode shape, like modulators based on slot waveguides [11]. Furthermore, the model presented here works for any kind of silicon modulator while the previous one works only for depletion based ones. The model proposed here uses the assumption (which is true for most of the silicon modulators in the literature) that carrier concentrations vary mainly in one direction when a voltage is applied on the structure. Thus the carrier concentration variations are modeled only in one direction (perpendicular to the plane of the junction in a case of a diode-based modulator). Carrier concentration profiles are then supposed to be uniform in the two other directions of space. As a major simplification, in the case of reverse biased PN diode, an analytical expression can be used to evaluate the carrier concentrations as a function of the applied voltage. Based on this assumption, the simplified model is schematized in Fig. 1(b). First the mode of the waveguide is calculated considering it passive i.e. there is no carriers in it. This is represented in Fig. 1(b) as the box "Modal Simulation". The results of this box are the electric fields ($E(x,y)$) and the effective index ($\mathrm{n_{eff}}$) of the modes. Secondly, a 1D simulation is used to model the electrical part: an analytical expression is used for reverse biased PN junctions, while classical semiconductor simulation software can be used in the other case, with the major simplification that only 1D simulation is required [12]. Carrier distributions along the junction direction are then extended in the other two directions of space in order to build a 3D carrier distribution ($n(x,y,z)$ and $p(x,y,z)$). Using the Soref model, these carrier distributions are transformed into refractive index changes. $\Delta\mathrm{n}(x,y,z)$ represents the change in the real part of the refractive index, and $\mathrm{k}(x,y,z)$ is the imaginary part of the refractive index. Finally, using perturbation theory for TE modes [13], efficiency and loss are deduced by:

$$\begin{aligned}\Delta\phi(L) &= \int_{z=0}^{L} \frac{2\pi}{\lambda} \frac{\iint \mathrm{n}(x,y)\,\Delta\mathrm{n}(x,y,z)\,|E_x(x,y)|^2\,dxdy}{\mathrm{n_{eff}} \iint |E_x(x,y)|^2\,dxdy} dz \\ IL_{\mathrm{dB}}(L) &= 20\log_{10}\left(\exp\left(\int_{z=0}^{L} \frac{2\pi}{\lambda} \frac{\iint \mathrm{k}(x,y,z)\,|E_x(x,y)|^2\,dxdy}{\iint |E_x(x,y)|^2\,dxdy} dz\right)\right)\end{aligned} \tag{1}$$

where $\Delta\phi(L)$ and $IL_{\mathrm{dB}}(L)$ are the phase shift and the loss in rad and dB respectively for a propagation length of L. $E_x(x,y)$ is electric component along the lateral dimension of the waveguide. λ represents the wavelength of operation, $\mathrm{n_{eff}}$ is the effective index of the passive waveguide and $\mathrm{n}(x,y)$ is the refractive index cross section of the waveguide. In comparison the complete simulation [see Fig. 1] requires a complex 2D/3D electrical simulation and a mode simulation for each voltage, while the simplified model requires only a simple 1D electrical simulation (analytical in the case of PN junction), one mode calculation and an overlap integral

Optics EXPRESS

for each voltage. The simplified model will drastically reduce the computation effort.

2.1. Model validation

In order to validate the model and assess its accuracy, a conventional carrier depletion phase modulator based on a lateral PN junction was chosen as benchmark [14, 15]. The modulator is sketched in Fig. 2. It is based on a 300nm thick SOI rib waveguide. The etching depth and the width of the waveguide were 150nm and 400nm, respectively. The P and N doping concentrations for both contacts were $5 \cdot 10^{17}\text{cm}^{-3}$. Finally the junction was offset 30nm towards the N part.

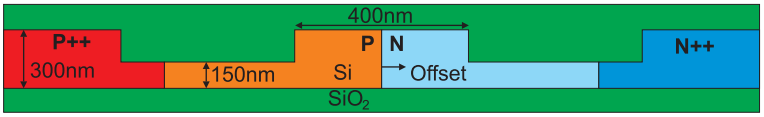

Fig. 2. Schematic view of the PN junction based modulator.

This modulator was simulated using both approaches (i.e. the complete simulation and the simplified model). Lumerical software suited was used to carry out the electrical and mode simulations [16]. Results are reported in Fig. 3, where efficiency and loss for L_π length are represented as a function of the reversed applied voltage. The simulation time for the simplified model was less than 5 minutes, which includes only one modal simulation and 33 overlap integrals because carriers distributions are calculated analytically. The complete simulation, however, took near 30 minutes, including a 2D Electrical Simulation of 33 voltage points and a modal simulation for each of those 33 voltage points. Very good agreement was obtained between both simulation approaches, therefore validating the simplified model approach. Efficiency of $V_\pi L_\pi = 1.53$Vcm and Loss of 5.3dB at 3V reverse applied voltage were calculated by the simplified model, which is less than 5% relative error compared to the complete simulation.

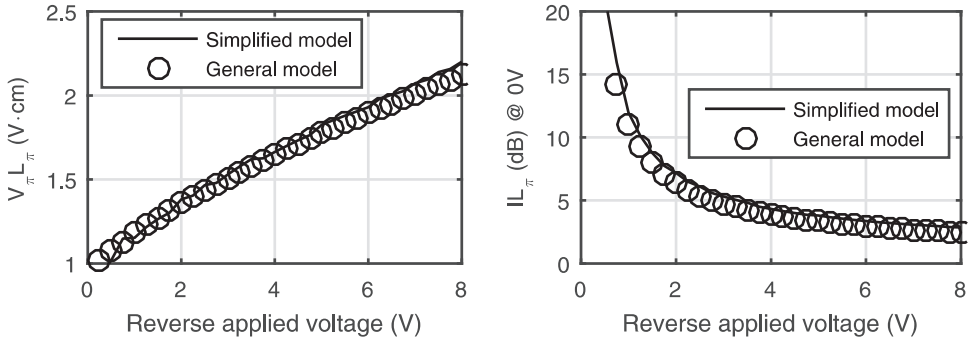

Fig. 3. Performance of the PN junction based modulator.

In PhoeniX OptoDesigner, the proposed model has been implemented. Physical mode simulations were performed to obtain effective index and loss versus voltage curve. Whereas the electrical part was modeled analytical, the optical part was fully simulated using a complex mode solver. Effective index and loss were calculated as a function of the applied voltage. These results were then fitted into a smooth function in order to create circuit models based on S-matrices.

Optics EXPRESS

3. Simulation of interdigitated PN junctions based silicon modulators

Modulators based on interdigitated PN junctions are normally considered as an option to further increase the efficiency of conventional depletion modulator based on lateral PN junctions, while maintaining good intrinsic bandwidth. This kind of modulator consists on periodically introducing PN junctions along the propagation direction, so that the overlap between the mode and the depletion zone is maximized. A schematic view is represented in Fig. 4. Even though several experimental demonstrations of this kind of modulators have been reported [17–19], its modeling remains a challenge because of the 3D nature of the structure. The memory requirement for a single simulation usually are in the order of tens of gigabytes, while the simulation times are around a few days. These computation constraints make it almost impossible to optimize this kind of modulators. In this purpose we used the same 300nm thick SOI technology used for the validation of the model, the etching depth and the width of the rib waveguide were chosen to be 250nm and 400nm respectively [see Fig. 4].

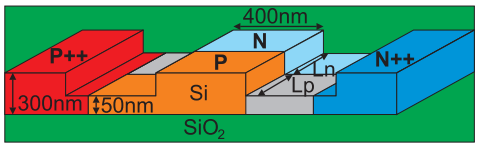

Fig. 4. Schematic view of the PN interdigitated junction based modulator.

The simplified model was applied to this structure. In this case, the carrier concentration varies in the propagation direction. Since junctions are PN, we modeled the carriers concentrations analytically. In order to implement the simplified model it is necessary to analyze a period of the interdigitated structure. Looking at a single period it is possible to identify three different zones; the N zone, the P zone and the depletion (intrinsic) zone in between. The length of the depletion zone changes according to the reverse applied voltage. However, the cross-section doping conditions remains in each of the three device zones. The perturbation theory was then employed in the three zones and the accumulated phase shift per period was calculated as a function of the applied voltage. The simplified model was then employed to optimize doping concentrations (P and N) and fingers lengths (L_P and L_N). Around 35000 sets of values were swept maintaining the total computation time below 5 hours. This was possible because the PN junctions are modeled analytically. Results predicted compromise values of good efficiency and reduced loss for $P = N = 8 \cdot 10^{17}\text{cm}^{-3}$ and $L_P = L_N = 200\text{nm}$ for doping concentrations and fingers length respectively. A complete simulation was carried out for this set of values, two other simulations were also carried out for two additional doping concentrations. Each simulation took around 30 hours of computing, mainly because of the 3D electrical simulation. Results of the complete simulations, along with simplified model ones, are represented in Fig. 5. There is good agreement between them. Moreover, trends are conserved between the complete simulation and the simplified model, which is very important from the design point of view. However a small difference can be observed in the efficiency. The reported values of the simplified model for efficiency and loss at 3V were $V_\pi L_\pi = 0.6\text{Vcm}$ and $\text{Loss} = 2.65\text{dB}$, while complete simulation reported $V_\pi L_\pi = 0.7\text{Vcm}$ and $\text{Loss} = 3.2\text{dB}$ ($P = N = 8 \cdot 10^{17}\text{cm}^{-3}$). This difference is mainly due to edge effects on the sides of the waveguide. There are two main source of errors; first the slab region is only 50nm thick representing a big difference from the analytical PN model used. Second, depletion zones in the simplified model were assumed abrupt in the propagation direction, while in the complete simulation they have rounded tips. However, it is important to point out that in this case the reduction in computation time is over 100 times. The calculated relative error was below 20%, representing a low error given the complexity of the problem and the reduction in computation time.

Optics EXPRESS

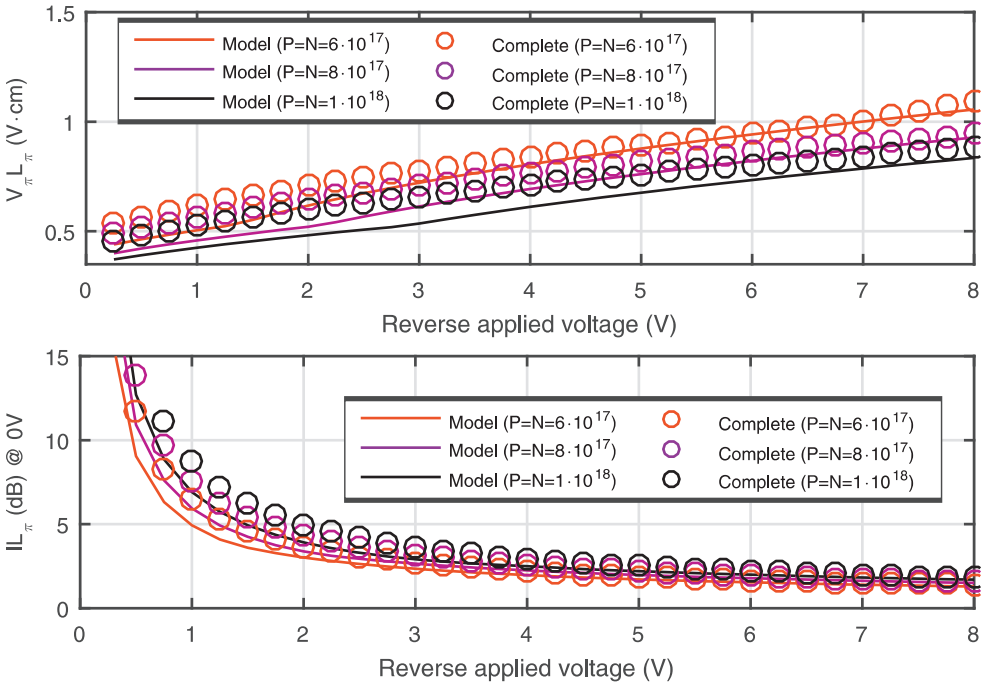

Fig. 5. Performance of the PN interdigitated junction based modulator.

4. Conclusion

In conclusion, simulations of modulators require in most cases many computational resources and computation time, reducing the ability of the designer to fully optimized the device. We have proposed and validated a simplified model that reduce those constraints, maintaining a good level of accuracy at the same time. This model has been implemented in Phoenix Optodesigner software with good results. We have also demonstrated how the model can be applied to the modulator based on PN interdigitated junctions allowing its optimization. These results demonstrate that the proposed model is a valuable tool to design and optimized silicon modulators.

Funding

French National Research Agency (ANR), project Ultimate (ANR-11-INFR-0015); European Commission, project Plat4m (FP7-2012-318178).